Geoscience Frontiers 11 (2020) 429–438

HOSTED BY

Contents lists available at ScienceDirect

China University of Geosciences (Beijing)

Geoscience Frontiers

journal homepage: www.elsevier.com/locate/gsf

Research Paper

Cyclic liquefaction screening of sand with non-plastic fines: Critical state approach

Md. Mizanur Rahman [a,*], T.G. Sitharam [b]

[a] Natural and Built Environments Research Centre (NBERC), School of Natural and Built Environments, University of South Australia, Mawson Lakes, SA 5095, Australia

[b] Department of Civil Engineering, Indian Institute of Science (IISc), Bangalore, India

ARTICLE INFO

Article history:
Received 4 January 2018
Received in revised form
2 April 2018
Accepted 18 September 2018
Available online 3 November 2018

Keywords:
Critical state
State parameter
Liquefaction
Sands
Fines
Constitutive model

ABSTRACT

There have been significant advances in the application of critical state, CS, in liquefaction potential assessment. This was done by comparing state parameter, ψ with estimated characteristic cyclic stress ratio, CSR due to an earthquake. A cyclic resistance ratio, CRR curve, which can be determined from cyclic liquefaction tests, separates historical liquefied and non-liquefied data points (ψ, CSR). On the other hand, the concepts of equivalent granular state parameter, ψ^*, which was developed for sands with fines, can be used in lieu ψ to provide a unifying framework for characterizing the undrained response of sands with non/low plasticity fines, irrespective of fines content (f_c). The present work combines these two propositions, and by merely substituting ψ^* for ψ into the aforementioned CS approach to capture the influence of f_c. A series of static and cyclic triaxial tests were conducted, separately and independently of the concept of ψ^*, for sand with up to f_c of 30%. The clean sand was collected from Sabarmati river belt at Ahmedabad city in India which was severely affected during the Bhuj earthquake, 2001. The experimental data gave a single relation for CRR and ψ^* which was then used to assess liquefaction potential for a SPT based case study, where f_c varies along the depth. The prediction matched with the field observation.

1. Introduction

Liquefaction, one of the most disastrous forms of geotechnical failure, was first described by Terzaghi and Peck (1948) as the sudden change of a stable loose saturated sand to a flow-like failure, when triggered by slight disturbance. The damages due to liquefaction attracted attention of engineers and seismologists during the Fukui earthquake in 1948 and Nigaata earthquake in 1964, which developed the initial foundation for liquefaction screening and analysis protocol. A large number of variables associated with soil properties (e.g. density, confining stress, grain size, fines content), their role during liquefaction and the uncertainties associated with earthquake loading shaped the backbone of these screening protocols to an empirical form (Seed and Idriss, 1971). The initial screening protocol has been through several revisions (Youd et al., 2001; Boulanger et al., 2012), however the limitation of these empirical methods often recognized for new datasets and adjustment was reported in literature (Maurer et al., 2014). These lead, from time to time, disagreement among top practitioners in identifying a reliable approach e.g. dissonance between Seed (2010) and Idriss and Boulanger (2008) on un-conservative elimination of sites with regards to liquefaction hazard. There is also lack of consensus on the effect of non-plastic and plastic fines (particle size $\leq$ 0.075 mm) on liquefaction resistance. Majority of laboratory test data showed a decreasing liquefaction resistance with fines content (f_c) (Thevanayagam and Martin, 2002; Rahman et al., 2008), whereas a typical screening chart, as shown in Fig. 1, shows increasing liquefaction resistance with f_c for the same standard penetration test, SPT-*N* value (Youd et al., 2001). Significant research efforts are going on worldwide to better understand the complexity of the problem and yet awaiting for a well-accepted "final" screening protocol. Despite of the challenges, practitioners often have to follow a liquefaction screening protocol for mandatory major design requirement or for liquefaction damage recovery e.g. in the city of Christchurch, New Zealand. Therefore, a more

* Corresponding author. Fax: +61 (0)8 830. 25082.
E-mail address: Mizanur.Rahman@unisa.edu.au (Md.M. Rahman).
Peer-review under responsibility of China University of Geosciences (Beijing).

https://doi.org/10.1016/j.gsf.2018.09.009

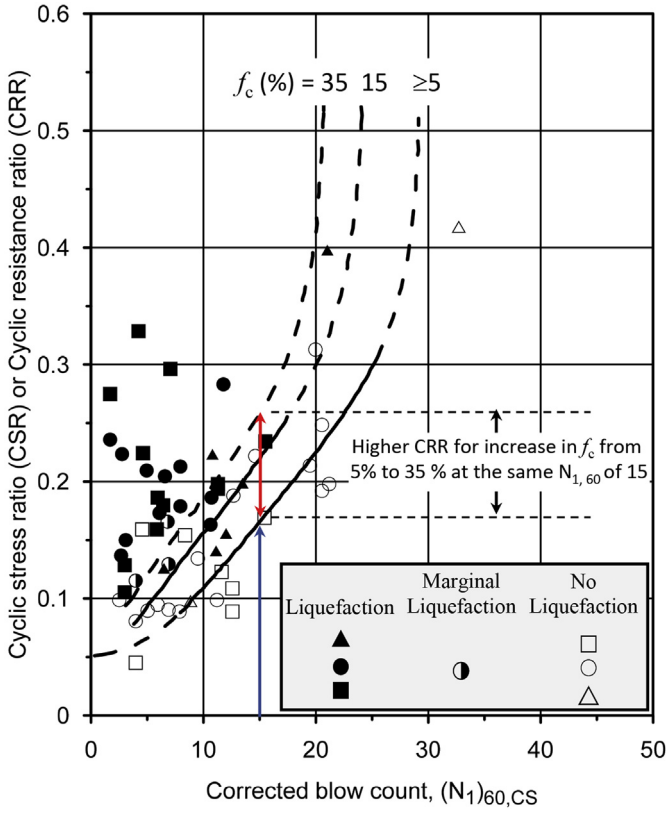

Figure 1. Liquefaction screening chart for SPT based liquefaction screening (data collected from Youd et al., 2001).

fundamental approach, alternative to empirical methods, is also in search. Recently, critical state soil mechanics (CSSM) is emerging in the literature as a promising pathway for liquefaction analysis for static (Carrera et al., 2011; Bedin et al., 2012) and cyclic (Bouckovalas et al., 2003; Huang and Chuang, 2011; Baki et al., 2014) loading, among them Jefferies and Been (2006) is the most comprehensive contribution. These studies used state parameter ψ, which is the difference between the current void ratio and the void ratio on the critical state (CS) line at the same mean effective stress (Been and Jefferies, 1985), as a key parameter for correlating liquefaction resistance for soil. The predicted resistance, from such relation, can be compared with expected stresses due to earthquake to assess liquefaction potential. The ψ at the filed condition can also be estimated from field tests e.g. cone penetration test (CPT), standard penetration test (SPT), shear wave velocity (V_s) (Been et al., 1986, 1987; Jefferies and Been, 2006; Shuttle and Cunning, 2007).

However, the CSSM has other challenges for the effect of fines. Experimental studies showed that an increase in f_c initially shifts the CSL downwards in e-log(p') space up to a threshold fines content (f_{thre}) (Thevanayagam et al., 2002); where e is void ratio and p' is effective confining stress. This becomes the main limitation as the individual CSL for each f_c has to be known to define ψ. Over the several decades, it was realized that e is not a consistent density index for the force structure of sand mixed with a range of f_c. Therefore, an equivalent granular void ratio, e^* was sought to capture the effect of f_c on mechanical behaviour, particularly CS behaviour. Initially, it was assumed that f_c has no contribution in sand force structure and therefore the f_c was considered as void in the conversion of e to e^* (Georgiannou et al., 1990; Ovando-Shelley and Pérez, 1997; Thevanayagam and Mohan, 2000). In early 90's, it was evident that a fraction of f_c has active role in the force structure (Pitman et al., 1994; Zlatovic and Ishihara, 1995) and Thevanayagam et al. (2002) proposed the following definition for e^* to consider the contribution of f_c.

$$e^* = \frac{e + (1-b)f_c}{1-(1-b)f_c} \quad (1)$$

where b represents the fraction of fines that are active in force structure of the sand skeleton. The e^* in conjunction with the b parameter coalesced the CSLs in e-log(p') space to a single trend line in e^*-log(p') space, irrespective of f_c, for many datasets (Thevanayagam et al., 2002; Ni et al., 2004; Yang et al., 2006; Rahman and Lo, 2008; Lashkari, 2014; Qadimi and Mohammadi, 2014). The single trend of CSLs is often called equivalent granular critical state line (EGCSL) which is used to modify state parameter, ψ to equivalent granular state parameter, ψ^* (Rahman and Lo, 2007). Recently, the ψ^* was correlated to mechanical behaviour (Rahman et al., 2014a; Mohammadi and Qadimi, 2015; Goudarzy et al., 2017) and constitutive model irrespective of f_c (Lashkari, 2014; Rahman et al., 2014b). However, there are different approaches to obtain b for e^* and this article is not focused on those but discusses the potential application of CS approach. Therefore, a brief description of b is presented in Appendix A. Since e and e^* are same for clean sand, the EGCSL does not need a separate formulation.

The objective of this article is to present a critical state (CS) approach for liquefaction assessment which is inspired by Jefferies and Been (2006), however extended to sand with fines which may not need separate CS framework for each f_c. This was done by merely substituting ψ^* for ψ into the CS approach. The testing materials were collected from affected area during Bhuj earthquake, 2001 in India and a CS framework was developed from a large number of laboratory triaxial tests. These tests were conducted by Dash (2008), independent of e^* and ψ^* formulation as described in appendix. However, these laboratory tests data showed a single trend of EGCSL when e was converted to e^*. The cyclic resistance ratio, CRR and ψ^* data points also exhibited an exponential relation of cyclic resistance. The SPT data of a site in Ahmedabad city, which was not liquefied during Bhuj earthquake, was converted to ψ. The f_c in the site was varied along the depth, therefore ψ was converted to ψ^*. Stresses due to Bhuj earthquake and ψ^* data points were then compared to cyclic resistance to assess liquefaction. The CS method predicted no liquefaction. The limitations of the CS method are recognized and authors hope that this article will trigger significant interest for further research on CS approach to overcome those limitations.

2. A review of the screening protocol and challenges for CSSM

2.1. Simplified liquefaction screening protocol

Whether a site would liquefy during an earthquake or not that can be assessed by comparing expected external stresses from an earthquake to resisting stress (strength) of the soil. A higher external stress (cyclic stress ratio, CSR) than resisting stress (cyclic resistance ratio, CRR) causes liquefaction. Seed and Idriss (1971) suggested a simplified procedure for estimating CSR from an earthquake as following:

$$CSR = \frac{\tau_{av}}{\sigma'_{vo}} = 0.65\left(\frac{\gamma h}{g}a_{max}\right)r_d\frac{1}{\sigma'_{vo}} = 0.65\left(\frac{a_{max}}{g}\right)\left(\frac{\sigma_{vo}}{\sigma'_{vo}}\right)r_d \quad (2)$$

$\gamma h a_{max}/g$ is the maximum shear stress on a rigid body due to peak ground acceleration; where γ is unit weight of the soil, h is the height of the soil column above the soil element, a_{max} is the peak

ground acceleration and τ_{av} is average shear stress due to earthquake. Seed and Idriss (1971) suggested an average ground acceleration would be 65% of a_{max} and reduction factor r_d as soil is a deformable body. For consistent comparison between case histories, the CSR in Eq. (2) commonly normalized for M_w of 7.5 by an earthquake magnitude scaling factor (MSF) and for effective overburden stress (Kσ). Thus, the average external stress, CSR induced by earthquake can be compared with soil resistance capacity by means of (i) historical evidence, and (ii) resistance determined by testing on high quality undisturbed specimens to assess liquefaction potential. It is customary to present both approaches in terms of field test data such as standard penetration test (SPT), cone penetration test (CPT), shear wave velocity (V_s) etc. In the first case, the field test data (say, SPT-*N* value), based on historical evidence whether or not a site have liquefied, are compared with CSR as shown in Fig. 1. This enabled to develop a narrow boundary between liquefied and non-liquefied sites. In the second case, cyclic resistance ratio ($CRR = \sigma_d/2\sigma'_0$) of undisturbed specimen recovered from a deposit were determined from laboratory element tests of known penetration resistance, *N* value. Then, comparing CRR (i.e. *N*) with CSR, it is possible to identify whether the site would liquefy or not during an earthquake which facilitate to the development liquefaction chart as shown in Fig. 1. Jefferies and Been (2006) suggested that this is "*a geological approach, rather than one based in mechanics*" as, with few other limitations, it does not properly consider mechanics of the effect of *e* and p' in CRR. However, the second case has a potential for the development of CSSM based screening protocol of liquefaction assessment.

2.2. Challenges for element tests and CSSM approach

The cyclic resistance of a soil element depends on its *e*, p', average magnitude of CSR and the number of cycles it may exposed due to an expected earthquake. This requires a large number of element tests on undisturbed specimen which is not feasible even for a large project. Alternatively, reconstitute specimens were used (Ishihara, 1993; Hyodo et al., 1998; Vaid et al., 2001), and correction applied for the difference between undisturbed and reconstitution. The current practice of testing procedure for cyclic resistance was demonstrated in Seed and Lee (1966) where they applied equal amplitude of axial stress to a saturated and consolidated (to a confining stress, p') soil element until they deform a certain level of peak to peak axial strain. It was found in many laboratory studies that the pore water pressure (pwp), Δu, developed to 90%–95% of p' at a 5% DA axial strain and it becomes a common practice to consider 5% DA as the initiation of liquefaction (Ishihara, 1993). The number of cycles, *N* required to achieve Δu of initial p' (equivalent 5% DA) depend on the applied CRR. For the same *e* and p', at least few tests are required to develop a CRR vs. *N* relation as shown in Fig. 2. The data were collected by Ishihara (1993) and Silver et al. (1976) which showed excellent repeatability for eight different laboratories. The relation can be presented by a trend line and will be referred as cyclic resistance (CR) curve hereafter. The CRR can be found from CR curve for an expected number of cycles, N_L from an earthquake. However, the N_L may depend on actual time history of acceleration during the earthquake. In reality, one should consider N_L that is relevant to the earthquake to estimate CRR and compare with CSR for liquefaction potential assessment. Seed and Idriss (1971) suggested 10, 20 and 30 cycles for M_w 7, 7.5 and 8 respectively. Ishihara (1993) also used 20 cycles for an earthquake of M_w 7.5. $N_L = 20$ is used for subsequent development in this study.

However, the above procedure requires a large number of tests for different densities, *e* and p' which may vary along the depth at the same site. Therefore, this would require indefinite number of tests to establish CR curve which is not practical. Therefore, this study hypothesised that the effect of density and p' on CRR of clean sand are captured by ψ as in Jefferies and Been (2006) and Huang and Chuang (2011). It is also hypothesised that the effect of non-plastic fines is captured by ψ^* as in Baki et al. (2012), Rahman et al. (2014b) and Lashkari (2016). This study combined these hypotheses and evaluated for liquefaction assessment within CSSM framework.

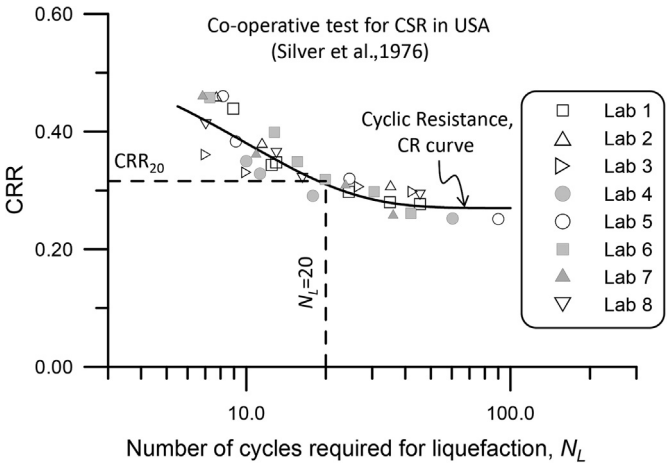

Figure 2. CR curve from Ishihara (1993) (data collected from Silver et al., 1976).

3. Experimental study

The Sabarmati river belt and the area surrounding Ahmedabad city in India were severely damaged due to liquefaction during the Bhuj earthquake, 2001 which killed 19,727 people and made 600,000 people homeless. The sand of this study was collected from excavated pits of a damaged site near the Sabarmati river belt. Then, the clean sand (SP) was prepared by wet sieving through a 75 μm sieve. It has a mean grain size D_{50} of 0.375 mm, uniformity coefficient (C_u) of 3.58, gradation coefficient (C_c) of 1.163. The particles are sub-angular to sub-rounded. A quarry dust (<75 μm) was used as fines. The fines have d_{50} of 0.037 mm and plasticity index (PI) of 1.57. The SEM photographs of sand and fines are shown in Fig. 3a,b. The sand and fines mixture were prepared by mixing clean sand with different percentage (by weight) of fines. The f_c covered in this experimental study was in the range of 0% to 30% with an incremental step of 5%. The grading size distribution curves for clean sand, fines and their mixtures are presented in Fig. 4. The specimens of this study were prepared by the dry deposition method, which is mostly representative of an aeolian deposit.

The experimental investigation was based on triaxial testing with fully automated data logging facilities. Axial load was measured with an internal submersible load cell. Transducers were used to measure vertical displacement, the volume change, chamber pressure, and excess pore water pressure. The loading system consists of a load frame and hydraulic actuator capable of performing both strain-controlled as well as stress-controlled dynamic tests with a frequency range of 0.01 Hz to 10 Hz, employing built-in sine, triangular and square wave forms. Strain controlled monotonic tests can also be performed with this loading system at a desired strain rate. The specimen dimensions were 50 mm in diameter and 100 mm in height. Saturation of the specimen was accomplished by CO_2 percolation followed by vacuum flushing under a small head, and back pressure application. A Skempton B-value of at least 0.95 was achieved in all the tests. A detail of the testing procedure can be found in Dash (2008).

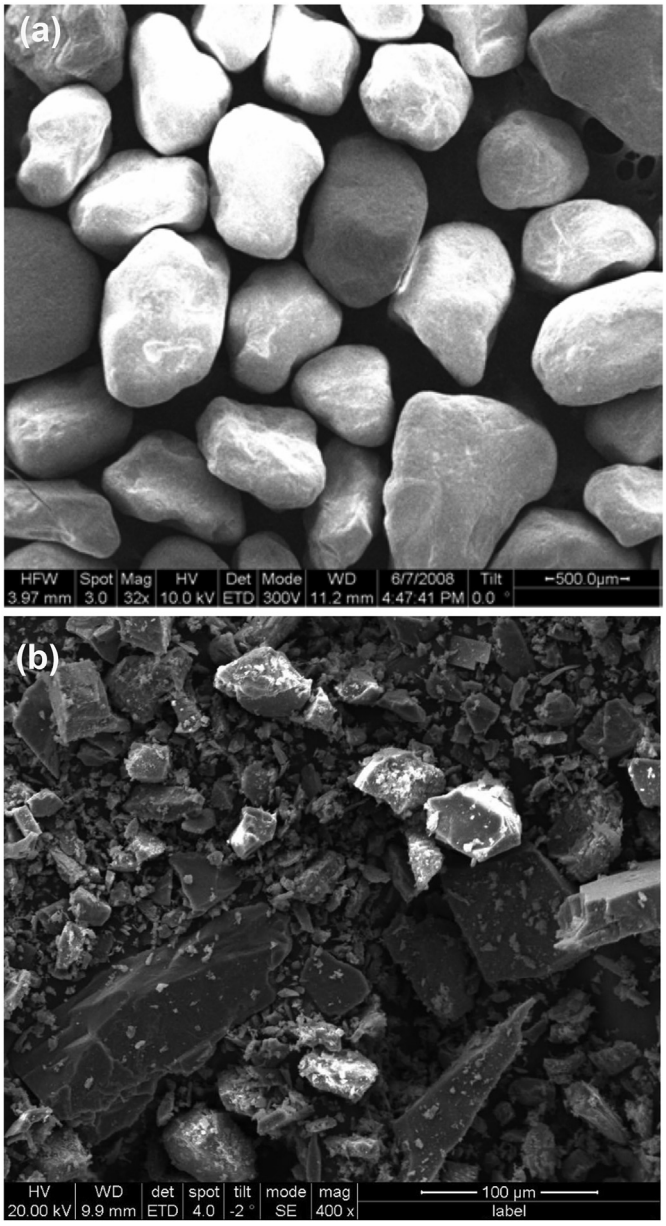

Figure 3. SEM photograph. (a) Clean sand; (b) fines (size ≤ 0.75 mm).

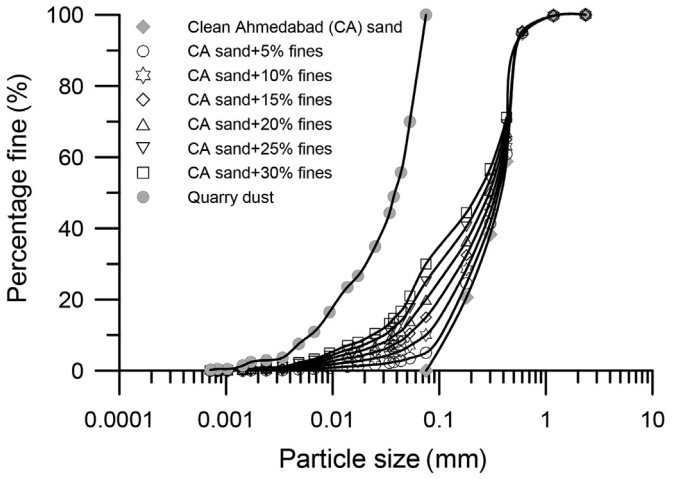

Figure 4. Grain size distribution curve for clean Ahmedabad sand, quarry dust and their mixture.

4. Undrained behaviour and EGCSL

4.1. Typical undrained behaviour: effect of f_c at same e_0

A series isotopically consolidated undrained monotonic triaxial tests were conducted for almost same e_0 but different f_c at p'_0 of 100 kPa; where the subscript '0' referred to the condition before shearing. A typical example of effective stress paths (ESPs), stress-strain paths and their development of pwp, Δu, for sand with 0% to 30% f_c, with 5% increment of f_c, for a similar void ratio, e_0 of ~0.540 are presented in Fig. 5a–c. Fig. 5a shows that the ESPs initially moved leftward then turn to the right to higher deviatoric stress, q (see inset zoom for clarity); a commonly observed behaviour for dilatant specimens. It was found that the deviatoric stress, q, at the peak or critical state decreased with increasing f_c up to 20%. Fig. 5b also shows this in q-ε_1 space. It was noticed that q increased again for f_c of 25% and 30%. The similar pattern was observed for pore water pressure development, Δu. A large negative Δu was developed for clean sand, however the rate of negative Δu was decreased with increasing f_c; a Δu almost equivalent to p'_0 of 100 kPa was obtained for f_c of 20% and then the rate of Δu were decreased again for f_c of 25% and 30%. Such changeover is often considered to occur at the threshold f_c. However, recent literature reported that the behaviour changeover does not occur at a threshold f_c, but over a transition zone and a threshold f_c is an idealized concept of behavioural change (Rahman et al., 2014b; Goudarzy et al., 2016).

However, most of these tests reached critical state toward the end of the tests at $dq = 0$, $dp' = 0$ and $du = 0$ when $d\varepsilon_1$ was a constant non-zero value (Dash et al., 2010). For tests that ended close to but not at CS, an objective extrapolation procedure can be used to obtain CS (Rahman and Lo, 2014; Zhang et al., 2018).

4.2. Equivalent granular critical state line, EGCSL

The Eq. (1) with the equation for b in the appendix was used to convert e to e^*. The equation for b has been evaluated with new emerging datasets by many researchers and general acceptability was observed (Lashkari, 2014; Mohammadi and Qadimi, 2015) and used in many other studies (Rahman and Lo, 2012, 2014; Baki et al., 2014). The D_{10} of host sand of 0.116 mm and d_{50} of fines of 0.037 mm were required in the conversion. With these values, the Eq. (9) in the appendix gave a f_{thre} of 31%, which was used in subsequent conversion of e to e^*. The CS data points, of 29 tests, were then plotted in the e^*-log(p') space as shown in Fig. 6. All the data points can be described by a single trend curve, referred to EGCSL, and can be presented by a power function.

$$e^* = e_{\lim} - \Lambda\left(\frac{p'}{p_a}\right)^{\xi} \quad (3)$$

where $e_{\lim} = 0.896$, $\Lambda = 92.5 \times 10^{-3}$ and $\xi = 0.70$. The EGCSL is used later as the anchor concept for the subsequent development of cyclic liquefaction behaviour screening protocol under the CSSM.

5. Cyclic liquefaction tests

5.1. Typical cyclic behaviour

A series isotropically consolidated undrained cyclic triaxial tests were conducted for different cyclic stress ratios (CSRs), e_0 and f_c at

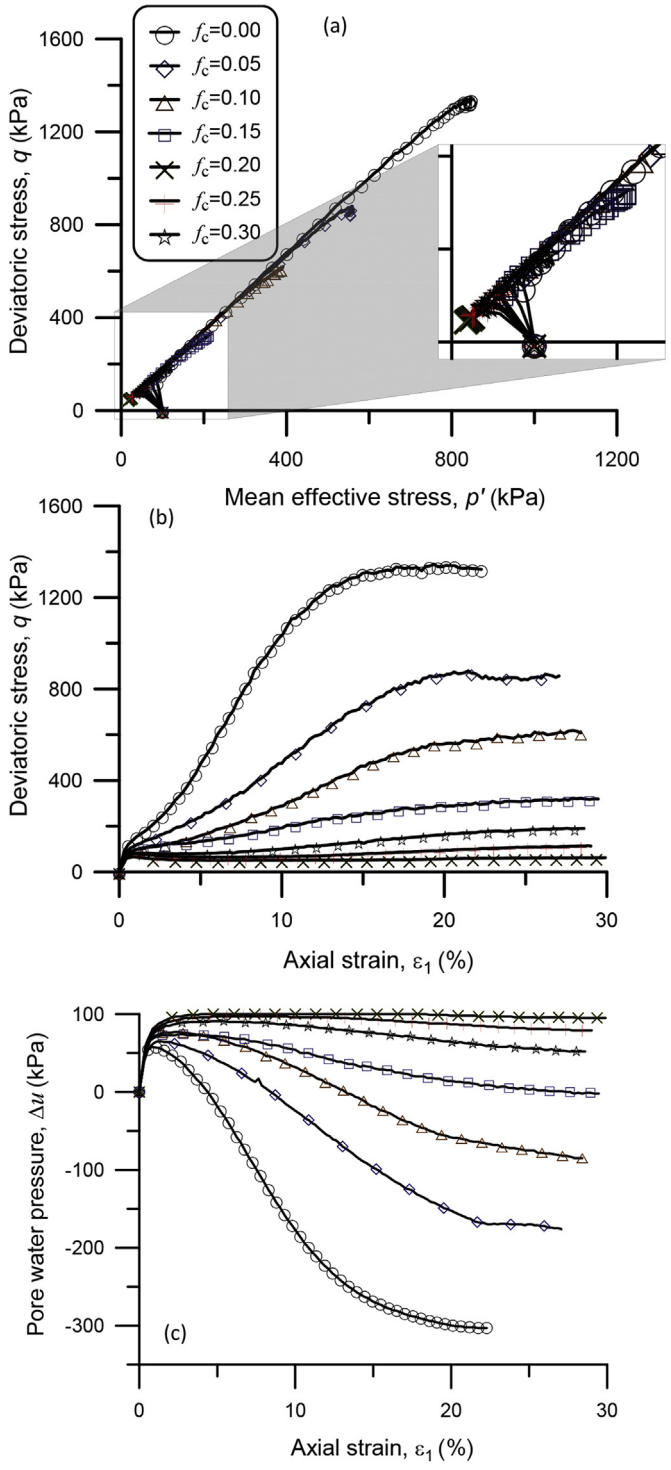

Figure 5. Typical undrained triaxial compression test results $e_0 \approx 0.50–0.54$. (a) ESPs; (b) stress-strain paths; and (c) development of pore water pressure.

p'_0 of 100 kPa. A typical example of effective stress paths, stress-strain paths and their development of pwp, Δu with cycles for sand with f_c of 5% for e_0 of 0.44 are presented in Fig. 7a–c. For CSR of 0.20, the ESP moved leftward with the cyclic pulses to form a butterfly shape toward a transient zero effective stress i.e. cyclic mobility. The number of cyclic pulses required to reach the initial zero effective stress was not exactly 5% DA axial strain as shown in red and blue lines in Fig. 7b. In this case, the Δu reached 100 kPa

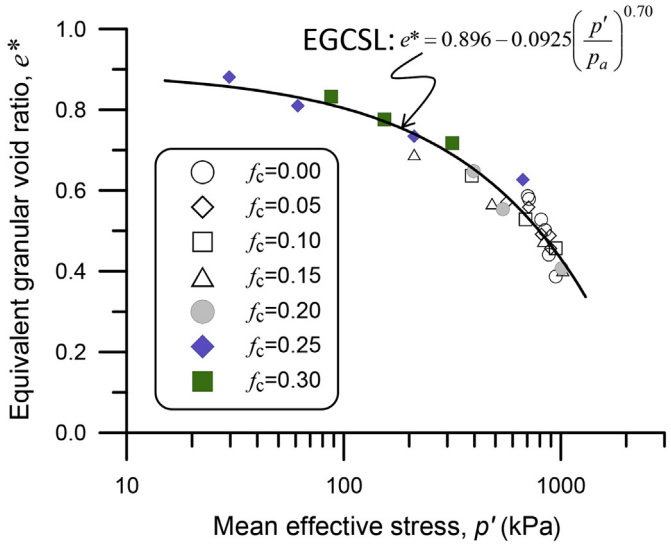

Figure 6. Equivalent granular critical state line (EGCSL).

(equal to p'_0) at N_L of 41. However in some cases, the Δu equaled to p'_0 was matched with 5% DA axial strain. In this study, the actual N_L required to reach Δu equal to p'_0 was considered as initial liquefaction for further analysis.

5.2. Cyclic stress ratio curve: effect of f_c

The data points for different CSRs and the N_L for a similar e_0 of ~0.54 and p'_0 of 100 kPa were plotted in Fig. 8 to obtain CR curve. The effect of f_c on CR curves, for sand with f_c from 0% to 30%, is presented in the figure. The CR curves moved downward with increasing f_c. The equivalent number of uniform significant cyclic stress pulse was assumed 20 for Bhuj earthquake of $M_w = 7.6$ in 2001 (Dash et al., 2010). Therefore, the CRR for 20 cycles, CRR_{20} can be obtained from Fig. 8 for N_L of 20. The CR relations gave seven CRR_{20} data points for seven different f_c. The process is repeated to obtain CRR_{20} for significantly different e_0. The relation between CSR_{20} and e_0 for different f_c is presented in Fig. 9a. The cyclic resistance of Ahmedabad sand in Sabarmati river belt to Bhuj earthquake or equivalent earthquake i.e. CRR_{20} decreased with increasing e_0 and f_c. The effect of f_c on CRR is opposite than that observed in the liquefaction screening chart in Fig. 1, where liquefaction resistance increases with f_c. Although this anomaly is attributed to the difference in testing conditions (Thevanayagam and Martin, 2002) and comparison basis (Carraro et al., 2003), further research is still required for better understanding. However, from CS point of view, scatter of these trends means that a large number of cyclic liquefaction tests are required for each f_c to characterize cyclic resistance (CRR) of a site with varying f_c.

The e_0 was converted to e^*_0 and plotted again in CSR_{20}-e^*_0 space. A single trend was observed which can be presented by the following equation

$$CSR_{20} = 12\exp(-8.5e^*_0) + 0.09 \quad (4)$$

Since the Eq. (4) is same for the clean sand and the sand with $f_c < f_{thre} = 0.31$, such a relation can be obtained from laboratory testing from clean sand only or sand with single f_c, which requires far less tests to characterize cyclic resistance of sand with f_c. However as discussed earlier, this relation would also be dependent on p'_0. Therefore, it is envisaged that both ψ and the equivalent granular state parameter, ψ^* can capture both the effect of e and p'.

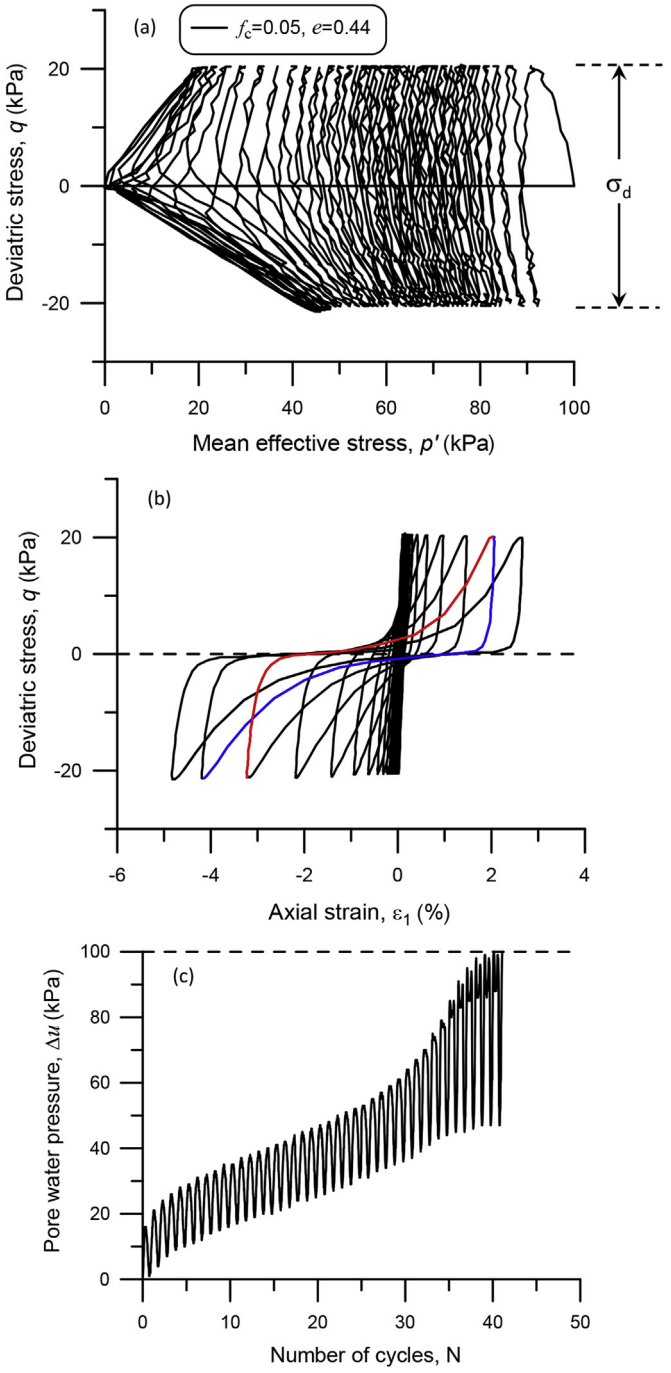

Figure 7. Typical cyclic liquefaction tests for CSR of 0.20 at $e_0 \approx 0.440$ and p'_0 of 100 kPa. (a) ESPs; (b) stress-strain paths; and (c) development of pore water pressure.

The ψ^* is a modified ψ by replacing CSL by EGCSL and e^* by e (Rahman and Lo, 2007), as following

$$\psi^* = e^* - \left[e_{\lim} - \Lambda\left(\frac{p'}{p_a}\right)^{\xi}\right] \quad (5)$$

The relation between ψ and ψ^* can be presented by the following equation

$$\frac{\psi}{\psi^*} = 1 - (1-b)f_c \quad (6)$$

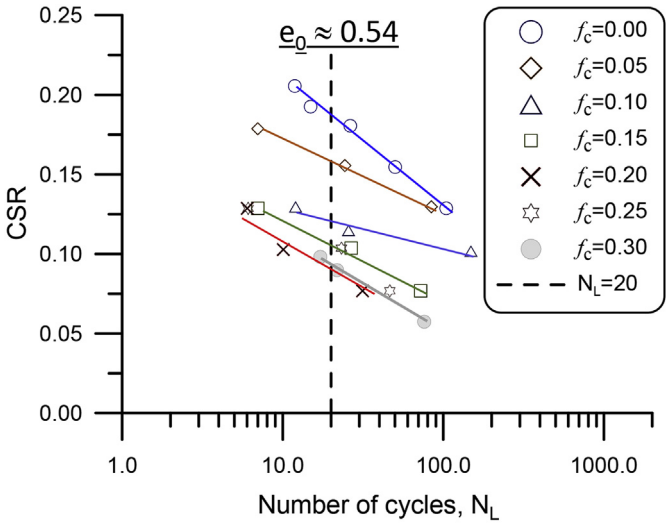

Figure 8. The effect f_c on the cyclic stress ration for $e_0 \approx 0.540$.

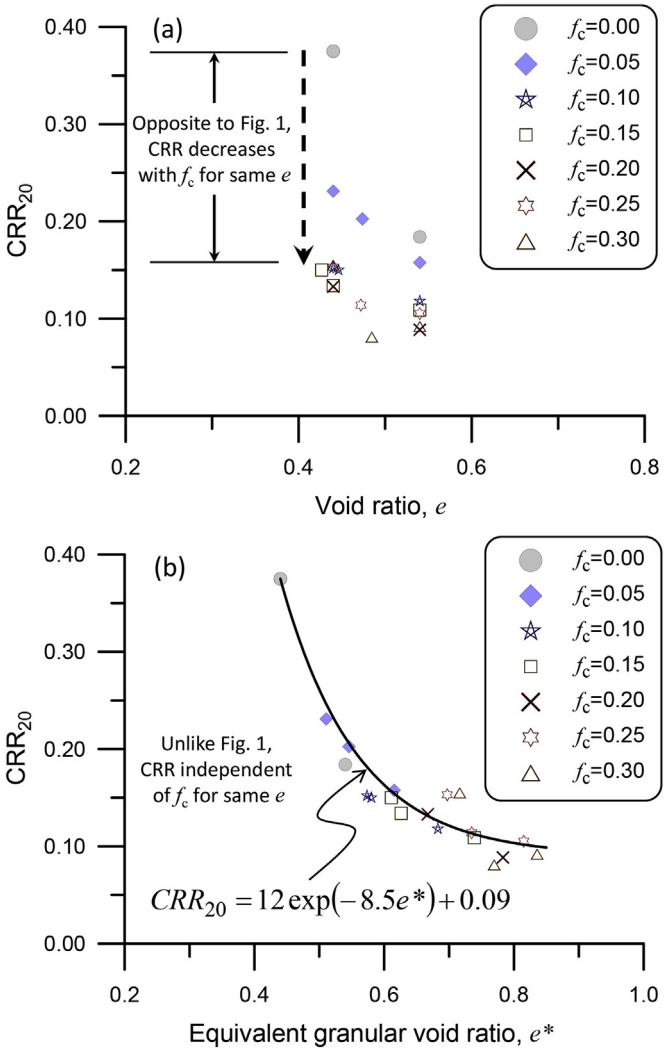

Figure 9. CRR for sand with fines. (a) CRR_{20} vs. e; (b) CRR_{20} vs. e^*.

where b can be obtained using the equations in the Appendix. The Eq. (6) readily converts ψ to ψ^* or vice versa. Since the EGCSL is same for all f_c, the CSL for clean sand or any one f_c can facilitate to obtain EGCSL as explained in Rahman and Lo (2008, 2014). Therefore, ψ or ψ^* for other f_c can be estimated using Eqs. (5) and (6). The CSR_{20}, for all f_c, are presented with ψ^* in Fig. 10. This gives a single trend line for a range of f_c. ψ^* was converted to ψ by Eq. (6) and plotted in Fig. 10b. A slight variation of the data points is observed, however their root-mean-square-deviation (RMSDs) and coefficient of correlation (R^2) remained almost same (see Fig. 10). Therefore, the overall trend can still be presented with the same equation

$$\begin{aligned} CRR_{20} &= 0.05\exp\left(-5\psi^*\right)+0.04 \\ &= 0.05\exp(-5\psi)+0.04 \end{aligned} \quad (7)$$

This is a useful correlation as ψ or ψ^* can be estimated from field test to estimate cyclic resistance capacity of Ahmedabad sand with fines to compare with exposed stress from Bhuj earthquake in 2001.

5.3. Discussion

There are a number of limitations of this study. The threshold fines content, f_{thre} was estimated as 31% which demarcates a "fines-in-sand" from a "sand-in-fines" matrix as an idealization of a transition zone. Since the concept of e^*, thus ψ^*, is only applicable for a "fines-in-sand" matrix, thus the proposed model, only works well for f_c below this transition zone. This transition zone may be narrow, ~2% either side of a distinct f_{thre} (Rahman and Lo, 2008), or may be "flat and wide" for another sand-fines mixture (Rahman et al., 2011), about 7% either side of a not-so-distinct f_{thre}. Readers should be aware of such variation of transition zone.

The effect of specimen preparation method and undisturbed/reconstitute specimen are discussed in earlier studies (Miura and Toki, 1982; Ishihara, 1993; Vaid et al., 1999; Huang and Chuang, 2011). The Eq. (7) has not been validated for sandy soil formed by other processes, therefore no adjustment was applied. This study was carried out for conventional liquefaction tests after isotopically consolidation specimens, whereas a level ground may likely be K0 consolidated. The effect of isotropic and K0 consolidation was not studied here, however reader can find recent literature (Nguyen et al., 2018; Rabbi et al., 2018; Rahman et al., 2018).

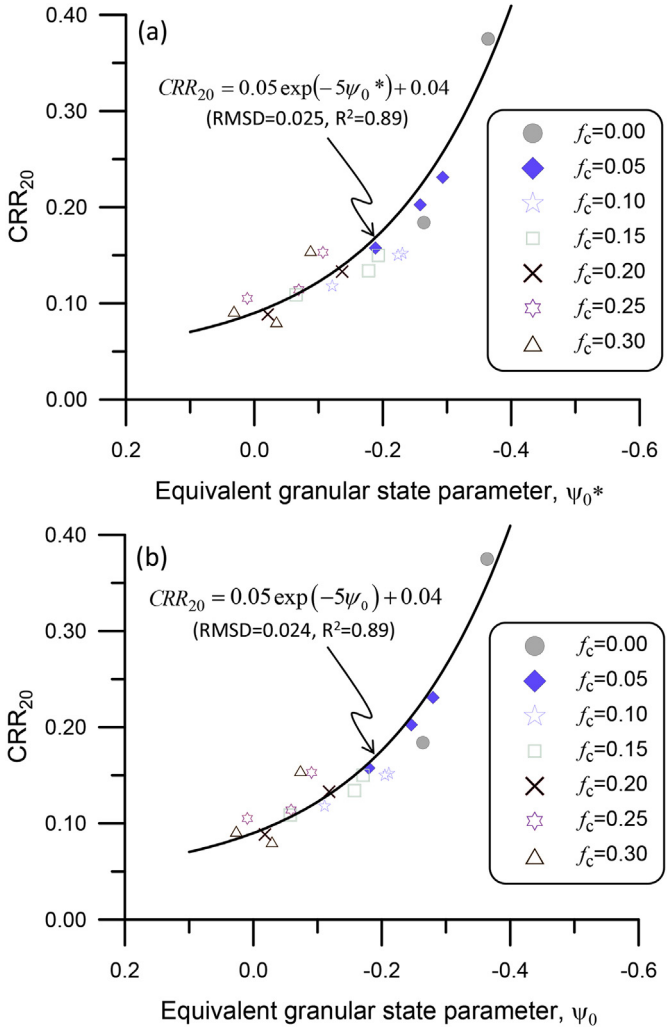

Figure 10. The relation between (a) CRR_{20} and ψ^*_0, and (b) CRR_{20} and ψ_0.

5.4. Published data sets

Three datasets extracted from literature: the most comprehensive dataset was obtained from Jefferies and Been (2006) for 15 sands with different specimen preparation methods, Maio Liao sand with f_c of 30% (Huang and Chuang, 2011), Fitzgerald Bridge Mixture (FBM) sand (Cubrinovski and Rees, 2008). It was noted that 15 sands by different specimen preparation methods, which supposedly have different initial fabric, did not show significant deviation/scatter. This could be due to the fabric independent nature of large strain behaviour such as CS (Li and Dafalias, 2012; Nguyen et al., 2017). The CRR_{20} and ψ^* of these datasets with the trend of Ahmedabad sand with fines are presented in Fig. 11. CRR_{15} was used for the dataset from Jefferies and Been (2006). An increasing upward trend of CRR with decreasing ψ^*_0, a similar trend as in Fig. 1, was observed irrespective of datasets. However, unique relation was not observed and this is expected as CRR should be related to the critical friction ratio e.g. $M_{CS} = (q/p')_{CS}$ (Jefferies and Been, 2006). Therefore, the parameters of Eq. (7) would be different for different sands or host sands. A future research should focus on normalizing CRR with an appropriate parameter to obtain a single relation.

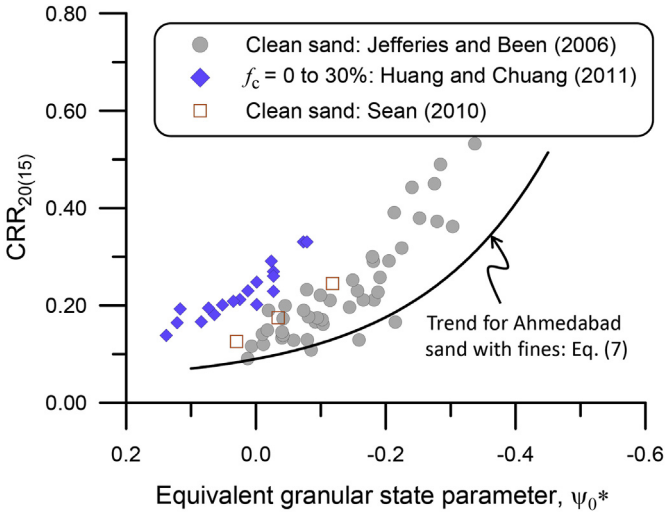

Figure 11. Relation between CSR and ψ^* (published data from Jefferies and Been, 2006; Huang and Chuang, 2011).

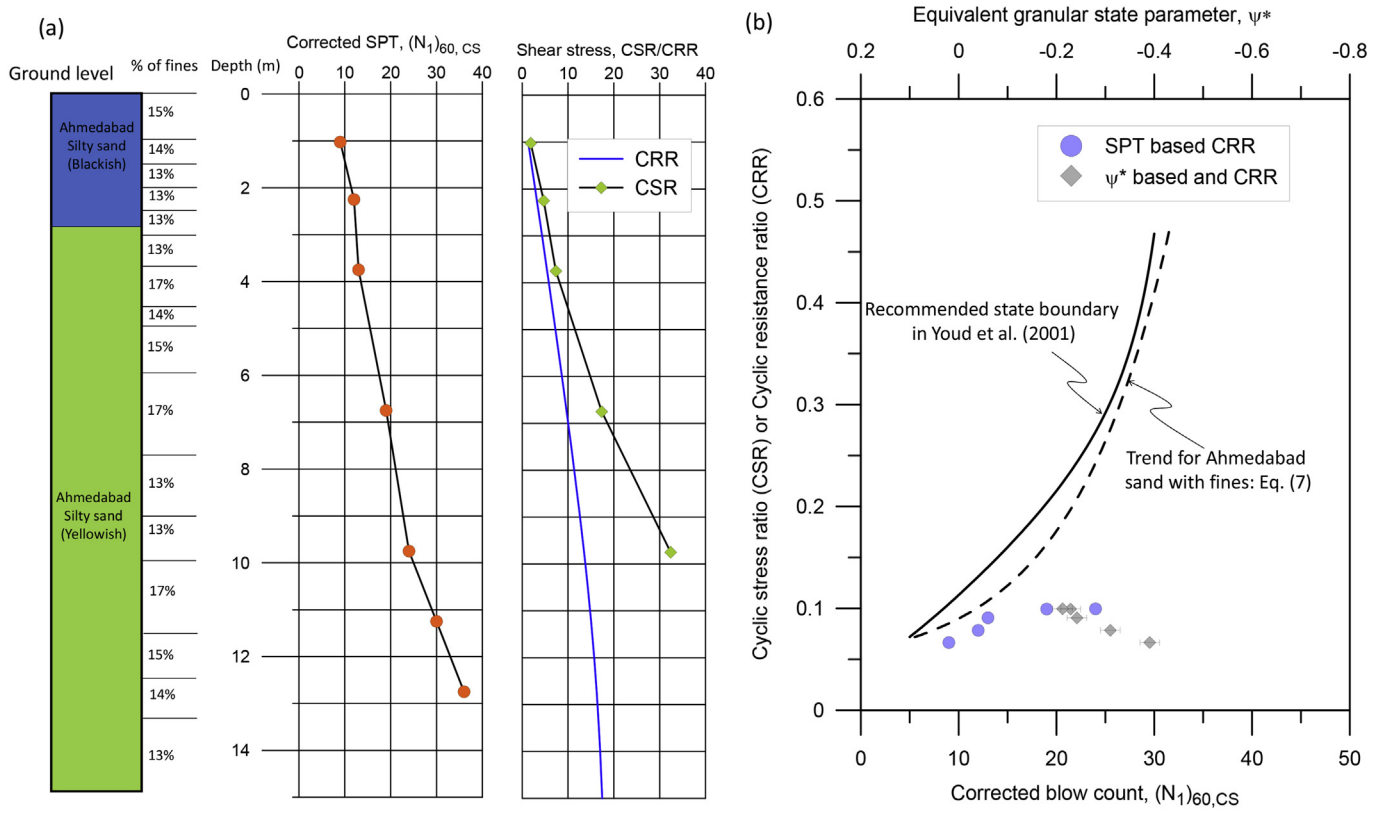

Figure 12. A case study of Sabarmati river site. (a) Soil profile and estimated CSR-CRR (Youd et al., 2001); (b) comparison of liquefaction assessment between Youd et al. (2001) and the CS approach.

6. Case study: a site close to sabarmati river

High quality field test data such as CPT in the Sabarmati rivers site were rare, however the soil exploration and SPT data from a non-liquefied site near Sabarmati rivers were collected from Raju et al. (2004) and shown in Fig. 12. The site exhibited different percentage of f_c mixed with Ahmedabad sand along the depth. The ground water table was assumed at 1.5 m below the surface and a_{max} of 0.106 was recorded at the ground floor of nearby passport office building (Raju et al., 2004). The corrected $(N_1)_{60,CS}$ and CRR-CSR are presented in Fig. 12a. The data was then presented in liquefaction screening chart as in Youd et al. (2001) and plotted right of the boundary curve i.e. predicted no liquefaction (Fig. 12b). This was consistent with the field observation and site response analysis. To apply CS approach to this site, the ψ has to be predicted from field SPT tests. There is no detailed study for predicting ψ for SPT N value; therefore, the relation between CPT and SPT was considered to obtain equivalent q_c from respective N value as detailed in the Appendix. The ψ values were estimated from q_c as discussed in Jefferies and Been (2006) and the relevant equations are presented in the Appendix. The CS data points up to p' of 300 kPa, in Fig. 6, can be assumed as straight line with a constant slope, λ of 0.14. The sand in the borelog has a variable f_c from 13% to 17% and therefore, it was assumed that soil type index, I_c would be in the range of 1.25 to 2.40. The range of I_c corresponded to a range of soils, from clean sand to silty sands. The range of I_c values, correspond a large range of soil type, gave a range of ψ values. The ψ values were then converted to a range of ψ^* values using Eq. (6). The range of ψ^* was presented by bar in Fig. 12b which also predicted 'no liquefaction'.

The above exercise inherently introduced some assumptions in the conversion from N_{60} to q_c and also has embedded limitation of estimating ψ from q_c. However, it shows a pathway to use CS framework for liquefaction screening using field test data. It is our intension that this article will generate sufficient research interest to evaluate and develop this CS approach.

7. Conclusions

This paper proposed a critical state (CS) approach for liquefaction assessment for sand with fines by combining two propositions: capturing of the influence of f_c with ψ^* (in lieu of ψ) and assessing liquefaction potential by comparing ψ with estimated characteristic cyclic stress ratio, CSR due to an earthquake. This was done by merely substituting ψ^* for ψ in CS approach (Jefferies and Been, 2006). A series of triaxial tests were conducted on sand collected from Sabarmati river belt at Ahmedabad city in India which was severely damaged during the Bhuj earthquake, 2001. The sand was washed to obtain clean Ahmedabad sand and mixed with 0% to 30% quarry dust with 5% increment. The experiments were done separately and independently of the concept of ψ^* development. The tests data are synthesized with ψ^* and the CS approach. The major findings of this study are:

(1) The critical state, CS data points for sand with up to f_c of 30% merged with CSL for clean sand when presented in e^*-log(p') space. This single trend line is referred to as EGCSL and was used as reference line to modify state parameter, ψ to equivalent granular state parameter, ψ^*.
(2) The cyclic resistance ratios at 20 cycles, CRR_{20} form a single relation with ψ^*, irrespective of f_c which can be presented by an exponential curve. The same exponential relation also represents CRR_{20} and ψ relation. However, the use of ψ^* may reduce the number of required tests in identifying CSLs for sand with each f_c.

(3) The CRR_{20} and ψ^* can be used to estimate liquefaction resistance for sand with f_c which can be compared with characteristic cyclic stress ratio, CSR of an earthquake to assess liquefaction potential. The CRR_{20} and ψ^* relation can be presented as liquefaction screening chart in Youd et al. (2001). Any data points (ψ^*, CSR) right of CRR_{20} and ψ^* relation represent non-liquefaction and vice-versa. The ψ^* may be estimated from field test. A SPT based case study of a site near Sabarmati river was used to assess liquefaction potential by the CS approach and compared with Youd et al. (2001). Both approaches predict no liquefaction which is consistent with the field observation.

Notwithstanding the above, the proposed model has a number of limitations as addressed in detail in the Discussion section.

Acknowledgement

The first authors would like to acknowledge the financial support for Australian Academy of Science Early Career Fellowship (RI 18.6) in 2012–2013 from the Australia-India Strategic Research Fund (AISRF) to visit Department of Civil Engineering, Indian Institute of Science, Bangalore, India to work for the background studies of this paper. He would like to acknowledge in-kind support from Indian Institute of Science, India and the University of South Australia, Australia for this study. We also acknowledge support from Dr. Suganya Kuppuswamy for SEM photo of fines for this study. The analysis in terms of e^* and the CS framework presented in this article are new and completely independent of earlier publications (Dash and Sitharam, 2009, 2011; Dash et al., 2010).

Notations

b	active fraction of fines in force structure of the soil skeleton
e	global void ratio
e^*	equivalent granular void ratio
ε_1	deviator strain
ψ	state parameter
ψ^*	equivalent granular state parameter
ψ^*_0	equivalent granular state parameter before shearing
f_c	fines content in decimal
f_{thre}	threshold fines content in decimal
p'	mean effective stress, $p' = (\sigma_1' + 2\sigma_3')/3$
q	deviator stress, $q = (\sigma_1' - \sigma_3')$
σ_1', σ_3'	major principal effectives stresses in triaxial condition

Appendix

Parameter b

The parameter, b in Eq. (1) represents the fraction of fines that are active in force structure of the soil skeleton. This physical meaning of b requires $1 \geq b \geq 0$. Earlier researches suggested $b \approx 0$. Such an approximation implies that the fines effectively function as void spaces. Such an approximation is only valid when f_c is low relative to f_{thre}. At higher f_c, $b \neq 0$. Rahman and Lo (2008), by re-analysing the experimental data of McGeary (1961) on binary packing studies and nine different sand-fines mixture from around the world, concluded that b is a function of both f_c and $\chi = D/d$, where D is the size of sand and d is the size of fines. Furthermore, the functional relationship, $b = F(f_c, \chi)$, has to possess a number of mathematical attributes (Rahman et al., 2008). To simulate the required attributes, Rahman and Lo (2008) proposed a semi-empirical equation expressed as below:

$$b = \left[1 - \exp\left(-0.3\frac{(f_c/f_{thre})}{k}\right)\right] \times \left(r\frac{f_c}{f_{thre}}\right)^r \quad (8)$$

where r = particle size ratio, D/d and $k = 1 - r^{0.25}$. Since sand and fines are generally not single-size materials, D/d was generalized to D_{10}/d_{50} based on the argument in Ni et al. (2004), where the subscripts denote fractile passing. The f_{thre} can be obtained from the experimental data, where available, as outlined in Rahman et al. (2009). However, as an initial approximation, f_{thre} can be taken as 0.30, but it may be determined more reliably using the following equation developed by Rahman et al. (2009).

$$f_{thre} = 0.40\left(\frac{1}{1 + e^{\alpha - \beta\chi}} + \frac{1}{\chi}\right) \quad (9)$$

The parameters α and β are determined by curve fitting to eight databases for χ in the range of 2 to 42, and this gave $\alpha = 0.50$ and $\beta = 0.13$.

Prediction ψ from SPT

Both CPT and SPT are penetration tests and there is close relationship between the measured resistance. Several researchers looked into this relation and the general form of this relation can be presented as following (Jefferies and Been, 2006):

$$q_c = \alpha N_{60} \quad (10)$$

The α is related to soil type index, I_c as suggested by Jefferies and Been (2006).

$$\alpha = 0.85\left(1 - \frac{I_c}{4.75}\right) \text{ MPa/blow} \quad (11)$$

The ψ can be determined from the following equation:

$$\psi = -\frac{\ln\left[\left(\frac{q_c - p}{p'}\right)\Big/k\right]}{m} \quad (12)$$

where $k = 8 + \frac{0.55}{\lambda - 0.01}$ and $m = 8.1 - 2.3\log(\lambda)$, λ slope of CSL.

References

Baki, M.A.L., Rahman, M.M., Lo, S.R., 2014. Predicting onset of cyclic instability of loose sand with fines using instability curves. Soil Dynamics and Earthquake Engineering 61–62, 140–151. https://doi.org/10.1016/j.soildyn.2014.02.007.

Baki, M.A.L., Rahman, M.M., Lo, S.R., Gnanendran, C.T., 2012. Linkage between static and cyclic liquefaction of loose sand with a range of fines contents. Canadian Geotechnical Journal 49 (8), 891–906. https://doi.org/10.1139/t2012-045.

Bedin, J., Schnaid, F., Da fonseca, A.V., Costa Filho, L.D., 2012. Gold tailings liquefaction under critical state soil mechanics. Géotechnique 62 (3), 263–267. https://doi.org/10.1680/geot.10.P.037.

Been, K., Crooks, J.H.A., Becker, D.E., Jefferies, M., 1986. The cone penetration test in sands: part I, state parameter interpretation. Géotechnique 36 (2), 239–249.

Been, K., Jefferies, M.G., 1985. A state parameter for sands. Géotechnique 35 (2), 99–112.

Been, K., Jefferies, M.G., Crooks, J.H.A., Rothenburg, L., 1987. The cone penetration test in sands: part II, general inference of state. Géotechnique 37 (3), 285–299.

Bouckovalas, G.D., Andrianopoulos, K.I., Papadimitriou, A.G., 2003. A critical state interpretation for the cyclic liquefaction resistance of silty sands. Soil Dynamics and Earthquake Engineering 23, 115–125.

Boulanger, R., Wilson, D., Idriss, I., 2012. Examination and reevalaution of SPT-based liquefaction triggering case histories. Journal of Geotechnical and Geoenvironmental Engineering 138 (8), 898–909. https://doi.org/10.1061/(ASCE)GT.1943-5606.0000668.

Carraro, J.A.H., Bandini, P., Salgado, R., 2003. Liquefaction resistance of clean and nonplastic silty sands based on cone penetration resistance. Journal of Geotechnical and Geoenvironmental Engineering 129 (11), 965–976.

Carrera, A., Coop, M., Lancellotta, R., 2011. Influence of grading on the mechanical behaviour of stava tailings. Géotechnique 61 (11), 935–946. https://doi.org/10.1680/geot.9.P.009.

Cubrinovski, M., Rees, S., 2008. Effect of fines on undrained behaviour of sands. In: Proc., 4th Decennial Geotechnical Earthquake Engineering and Soil Dynamics Conference, GSP-181. ASCE Sacramento, California, USA.
Dash, H.K., 2008. Undrained Cyclic and Monotonic Response of Sand-silt Mixtures. PhD thesis. Indian Institute of Science, Bangalore, India.
Dash, H.K., Sitharam, T.G., 2009. Undrained cyclic pore water pressure response of sand-silt mixtures:effect of non-plastic fines and other parameters. Geotechnical & Geological Engineering 27, 501–517. https://doi.org/10.2007/s10706-009-9252-5.
Dash, H.K., Sitharam, T.G., 2011. Undrained monotonic response of sand–silt mixtures: effect of nonplastic fines. Geomechanics and Geoengineering: International Journal 6 (1), 47–58. https://doi.org/10.1080/17486021003706796.
Dash, H.K., Sitharam, T.G., Baudet, B.A., 2010. Influence of non-plastic fines on the response of silty sand to cyclic loading. Soils and Foundations 50 (5), 695–704.
Georgiannou, V.N., Burland, J.B., Hight, D.W., 1990. The undrained behaviour of clayey sands in triaxial compression and extension. Géotechnique 40 (3), 431–449.
Goudarzy, M., Rahemi, N., Rahman, M.M., Schanz, T., 2017. Predicting the maximum shear modulus of sands containing non-plastic fines. Journal of Geotechnical and Geoenvironmental Engineering 143 (9), 1–5. https://doi.org/10.1061/(ASCE)GT.1943-5606.0001760.
Goudarzy, M., Rahman, M.M., König, D., Schanz, T., 2016. Influence of non-plastic fines content on maximum shear modulus of granular materials. Soils and Foundations 56 (6), 973–983. https://doi.org/10.1016/j.sandf.2016.11.003.
Huang, A.-B., Chuang, S.-Y., 2011. Correlating cyclic strength with fines contents through state parameters. Soils and Foundations 51 (6), 991–1001.
Hyodo, H., Hyde, A.F.L., Aramaki, N., 1998. Liquefaction of crushable soils. Géotechnique 48 (4), 545–553.
Idriss, I., Boulanger, R., 2008. Liquefaction during earthquakes." Earthquake Engineering Research Institute, Earthquake Engineering Research Institute, MNO-12.
Ishihara, K., 1993. Liquefaction and flow failure during earthquakes. Géotechnique 43 (3), 351–415.
Jefferies, M., Been, K., 2006. Soil Liquefaction: a Critical State Approach. Taylor & Francis, London. ISBN: 0-419-16170-8.
Lashkari, A., 2014. Recommendations for extension and re-calibration of an existing sand constitutive model taking into account varying non-plastic fines content. Soil Dynamics and Earthquake Engineering 61–62 (0), 212–238. https://doi.org/10.1016/j.soildyn.2014.02.012.
Lashkari, A., 2016. Prediction of flow liquefaction instability of clean and silty sands. Acta Geotechnica 1–28. https://doi.org/10.1007/s11440-015-0413-9.
Li, X., Dafalias, Y., 2012. Anisotropic critical state theory: role of fabric. Journal of Engineering Mechanics 138 (3), 263–275. https://doi.org/10.1061/(ASCE)EM.1943-7889.0000324.
Maurer, B., Green, R., Cubrinovski, M., Bradley, B., 2014. Evaluation of the liquefaction potential index for assessing liquefaction hazard in Christchurch, New Zealand. Journal of Geotechnical and Geoenvironmental Engineering 140 (7), 04014032. https://doi.org/10.1061/(ASCE)GT.1943-5606.0001117.
McGeary, R.K., 1961. Mechanical packing of spherical particles. Journal of the American Ceramic Society 44 (10), 513–522.
Miura, S., Toki, S., 1982. A sample preparation method and its effect on static and cyclic deformation-strength properties of sand. Soils and Foundations 22 (1), 61–77.
Mohammadi, A., Qadimi, A., 2015. A simple critical state approach to predicting the cyclic and monotonic response of sands with different fines contents using the equivalent intergranular void ratio. Acta Geotechnica 10 (5), 587–606. https://doi.org/10.1007/s11440-014-0318-z.
Nguyen, H.B.K., Rahman, M.M., Fourie, A.B., 2017. Undrained behaviour of granular material and the role of fabric in isotropic and K0 consolidations: DEM approach. Géotechnique 67 (2), 153–167. https://doi.org/10.1680/jgeot.15.P.234.
Nguyen, H.B.K., Rahman, M.M., Fourie, A.B., 2018. Characteristic behaviour of drained and undrained triaxial tests: a DEM study. Journal of Geotechnical and Geoenvironmental Engineering 144 (9), 04018060. https://doi.org/10.1061/(ASCE)GT.1943-5606.0001940.
Ni, Q., Tan, T.S., Dasari, G.R., Hight, D.W., 2004. Contribution of fines to the compressive strength of mixed soils. Géotechnique 54 (9), 561–569.
Ovando-Shelley, E., Pérez, B.E., 1997. Undrained behaviour of clayey sands in load controlled triaxial tests. Géotechnique 47 (1), 97–111.
Pitman, T.D., Robertson, P.K., Sego, D.C., 1994. Influence of fines on the collapse of loose sands. Canadian Geotechnical Journal 31 (5), 728–739.
Qadimi, A., Mohammadi, A., 2014. Evaluation of state indices in predicting the cyclic and monotonic strength of sands with different fines contents. Soil Dynamics and Earthquake Engineering 66 (0), 443–458. https://doi.org/10.1016/j.soildyn.2014.08.002.
Rabbi, A.T.M.Z., Rahman, M.M., Cameron, D.A., 2018. Undrained behavior of silty sand and the role of isotropic and K0 consolidation. Journal of Geotechnical and Geoenvironmental Engineering 144 (4), 04018014. https://doi.org/10.1061/(ASCE)GT.1943-5606.0001859.
Rahman, M., Baki, M., Lo, S., 2014a. Prediction of undrained monotonic and cyclic liquefaction behavior of sand with fines based on the equivalent granular state parameter. International Journal of Geomechanics 14 (2), 254–266. https://doi.org/10.1061/(ASCE)GM.1943-5622.0000316.
Rahman, M.M., Lo, S.-C.R., Dafalias, Y.F., 2014b. Modelling the static liquefaction of sand with low-plasticity fines. Géotechnique 64 (11), 881–894. https://doi.org/10.1680/geot.14.P.079.
Rahman, M.M., Lo, S.R., 2007. Equivalent granular void ratio and state parameters for loose clean sand with small amount of fines. In: Proc., 10th Australia New Zealand Conference on Geomechanics: Common Ground, 21-24 Oct 2007, Brisbane, Australia, pp. 674–679.
Rahman, M.M., Lo, S.R., 2008. The prediction of equivalent granular steady state line of loose sand with fines. Geomechanics and Geoengineering 3 (3), 179–190. https://doi.org/10.1080/17486020802206867.
Rahman, M.M., Lo, S.R., 2012. Predicting the onset of static liquefaction of loose sand with fines. Journal of Geotechnical and Geoenvironmental Engineering 138 (8), 1037–1041. https://doi.org/10.1061/(ASCE)GT.1943-5606.0000661.
Rahman, M.M., Lo, S.R., 2014. Undrained behaviour of sand-fines mixtures and their state parameters. Journal of Geotechnical and Geoenvironmental Engineering 140 (7), 04014036. https://doi.org/10.1061/(ASCE)GT.1943-5606.0001115.
Rahman, M.M., Lo, S.R., Baki, M.A.L., 2011. Equivalent granular state parameter and undrained behaviour of sand-fines mixtures. Acta Geotechnica 6 (4), 183–194. https://doi.org/10.1007/s11440-011-0145-4.
Rahman, M.M., Lo, S.R., Gnanendran, C.T., 2008. On state behaviour of loose sand with fines. Canadian Geotechnical Journal 45 (10), 1439–1456. https://doi.org/10.1139/T08-064.
Rahman, M.M., Lo, S.R., Gnanendran, C.T., 2009. Reply to discussion by Wanatowski, D. and Chu, J. on- on equivalent granular void ratio and steady state behaviour of loose sand with fines. Canadian Geotechnical Journal 46 (4), 483–486. https://doi.org/10.1139/T09-025.
Rahman, M.M., Nguyen, H.B.K., Rabbi, A.T.M.Z., 2018. The effect of consolidation on undrained behaviour of granular materials: a comparative study between experiment and DEM simulation. Geotechnical Research 5 (4), 199–217.
Raju, L.G., Ramana, G.V., Rao, C.H., Sitharam, T.G., 2004. Site specific ground response analysis. Geotechnics and Earthquake Hazaeds 87 (10), 1354–1362.
Seed, H.B., 2010. Technical Review and Comments: 2008 EERI Monograph Title Soil Liquefaction during Earthquakes. University of California, Berkeley. Geotechnical Report No, UCB/GT-2010/01.
Seed, H.B., Idriss, I.M., 1971. Simplefied prodecure for evaluating soil liquefaction potential. Journal of the Soil Mechanics and Foundation Division, ASCE 97 (9), 1249–1273.
Seed, H.B., Lee, K.L., 1966. Liquefaction of saturated sands during cyclic loading. Journal of Soil Mechanics and Foundation Division, ASCE 92 (SM6), 105–134.
Shuttle, D.A., Cunning, J., 2007. Liquefaction potential of silts from CPTu. Canadian Geotechnical Journal 44 (1), 1–19. https://doi.org/10.1139/t06-086.
Silver, M.L., Wilson, J.H., Valera, J.E., Townsend, F.C., Tiedemann, D.A., Lee, K.L., Ladd, R.S., Chan, C.K., 1976. Cyclic triaxial strength of standard test sand. Journal of the Geotechnical Engineering Division, ASCE 102 (5), 511–523.
Terzhagi, K., Peck, R.B., 1948. Soil Mechanics in Engineering Practice, Chichester. Wiley.
Thevanayagam, S., Martin, G.R., 2002. Liquefaction in silty soils-screening and remediation issues. Soil Dynamics and Earthquake Engineering 22 (9–12), 1035–1042.
Thevanayagam, S., Mohan, S., 2000. Intergranular state variables and stress-strain behaviour of silty sands. Géotechnique 50 (1), 1–23.
Thevanayagam, S., Shenthan, T., Mohan, S., Liang, J., 2002. Undrained fragility of clean sands, silty sands, and sandy silts. Journal of Geotechnical and Geoenvironmental Engineering 128 (10), 849–859.
Vaid, Y.P., Sivathayalan, S., Stedman, D., 1999. Influence of specimen-reconstituting method on the undrained response of sand. Geotechnical Testing Journal 22 (3), 187–195.
Vaid, Y.P., Stedman, J.D., Sivathayalan, S., 2001. Confining stress and static shear effects in cyclic liquefaction. Canadian Geotechnical Journal 38 (03), 580–591.
Yang, S.L., Sandven, R., Grande, L., 2006. Steady-state lines of sand-silt mixtures. Canadian Geotechnical Journal 43 (11), 1213–1219.
Youd, T.L., Idriss, I.M., Andrus, R.D., Arango, I., Castro, G., Christian, J.T., Dobry, R., Finn, W.D.L., Harder, L.F., Hynes, M.E., Ishihara, K., Koester, J.P., Liao, S.S.C., Marcuson, W.F., Martin, G.R., Mitchell, J.K., Moriwaki, Y., Power, M.S., Robertson, P.K., Seed, R.B., Stokoe, K.H., 2001. Liquefaction resistance of soils: summary report from the 1996 NCEER and 1998 NCEER/NSF workshops on evaluation of liquefaction resistance of soils. Journal of Geotechnical and Geoenvironmental Engineering 127 (10), 817–833.
Zhang, J., Lo, S.-C.R., Rahman, M.M., Yan, J., 2018. Characterizing monotonic behavior of pond ash within critical state approach. Journal of Geotechnical and Geoenvironmental Engineering 144 (1), 04017100. https://doi.org/10.1061/(ASCE)GT.1943-5606.0001798.
Zlatovic, S., Ishihara, K., 1995. On the influence of nonplastic fines on residual strength. In: Proc., Proceedings of IS-TOKY0'95/the First International Conference on Earthquake Geotechnical Engineering/Tokyo/14-16 November 1995. A.A. Balkema, Rotterdam, Tokyo, Japan, pp. 239–244.